Gas - escape features along the Trzebiatów Fault offshore Poland: evidence for a leaking petroleum system

Quang Nguyen[1*], Michal Malinowski[1,2], Regina Kramarska[3], Dorota Kaulbarsz[3], Leslaw Mil[3], Christian Hübscher[4]

[1] Institute of Geophysics, Polish Academy of Sciences, Warsaw

[2] Geological Survey of Finland, Espoo

[3] Polish Geological Institute – National Research Institute, Maritime Geology branch, Gdańsk

[4] Institute of Geophysics, University of Hamburg, Hamburg

Abstract: New 2D high resolution seismic and hydro-acoustic data demonstrate the presence of methane in the shallow sediments and its origin in the Pomeranian Bight, southern of the Baltic Sea area. Various shallow gas features including chimneys, bright spots, acoustic blanking, pockmarks, and polarity reversal were identified in the Gryfice block, along the inverted Trzebiatów fault zone. Structural and stratigraphic interpretation with support of seismic attributes shows the potential of fluid migration pathways from the Upper Triassic formation reservoirs to shallow sediments below the seafloor. It also helps in the explanation of how this natural gas escapes to the sea bottom. Amplitude-vs-offset (AVO) analysis proved free gas existence in the potential Upper Triassic reservoir, and helped locate free gas deposits within sediments. Hydro-acoustic data illustrated the gas chimneys' anomalies and corresponding free gas accumulation in Pleistocene to Quaternary successions. Leaking of gas to the seafloor was also proved by exposure of pockmarks on multibeam (bathymetry) data at the seafloor. We combine seismic, hydro-acoustic data and information on petroleum system from previous studies to explain signatures of free gas and its migration from lower reservoirs to shallow sediments.

Keywords: reflection seismic, hydro-acoustics, fluid escape, shallow gas, petroleum system

1. Introduction

Methane (CH_4) is the most abundant gas accumulated in shallow sediments compared to carbon dioxide, hydrogen sulfide, and higher chain hydrocarbon. Gas (hydrocarbons in general) can originate from either biological or thermogenic processes. While the biogenic gas is generated by bacterial activity mainly within a few meters of sediments (Parkes et al, 1990), the thermogenic gas is derived from organic materials at

* Corresponding author. Institute of Geophysics, Polish Academy of Sciences, Warsaw, Poland.
Email address: qnguyen@igf.edu.pl (Quang Nguyen)

high pressures and temperatures and frequently at depths of more than 1000 m (Floodgate and Judd, 1992). Thermogenic gas often migrates to the seafloor and is trapped in shallow sediments. The presence of shallow gas impacts both the geosystem and various ecosystems: e.g., geohazards related to the stability of the offshore infrastructure (Fleischer et al., 2001; Hovland et al., 1993; Naudts et al., 2009) or drilling offshore oil and gas wells (Adams and Kuhlman, 1991; Schroot and Schüttenhelm, 2003; Ren et al., 2019), as well as water chemistry and flora and fauna habitats (Idczak et al. 2020; Judd and Hovland, 2009).

Free gas presence in shallow marine sediments can be recognized in seismic and hydro-acoustic data by some distinct signal appearance (Conti et al., 2002; Dondurur et al., 2011; Kim et al., 2020; Aiello and Caccavale, 2022). Acoustic turbidity or acoustic blanking are seismic frequency-related features due to scattering and absorption of seismic energy in gas-charged areas (Hovland and Judd, 1988; Woodside et al., 1998; Donda et al., 2019). While acoustic turbidity appears as chaotic/discontinuous reflections, being mostly found in pockmark areas, acoustic blanking represents the absence of reflections beneath gassy layers (Mathys et al., 2005; Tóth et al., 2014). Acoustic blanking is one of the most common gas-related features, it appears as a smear zone where reflections are faint and absent at a certain level (Judd and Hovland, 2009; Schroot et al., 2005). This may be caused by the migration of free gas or the reflection of acoustic energy by overlapping hard sediment (Judd and Hovland, 1992). Gas accumulation areas can also cause amplitude bright spots which usually occur at a depth of more than 100 m and possibly at relatively high pressure (Hovland and Judd, 1988). Bright reflectivity zones often form reverberations or ringing in acoustic data (Davy, 1992; Tóth et al., 2014). They are similar to bright spots but occur in shallower records. These features are frequently observed together with acoustic turbidity zones (Judd and Hovland, 1992). Decrease in seismic velocity and lower density in gas-charged sediments can also cause a polarity reversal of the corresponding reflections (Garcia-Gil et al., 2002; Kim et al., 2020).

Mechanisms and processes of the free gas migration from sediments to the earth's surface can be classified as continuous or discontinuous types of migration (Khilyuk et al., 2000). Continuous migration occurs when there is an unbroken saturation of gas from the source to the surface. Gas flows from a higher pressure area to a lower pressure area, the flow rate of gas is directly related to the pressure drop along the migration path. There are two potential pathways for this type of migration either natural occurring pathway as fracture or fault, or man-made pathway such as drilled boreholes (Yang et al., 2017; Bruin et al., 2022). The discontinuous migration occurs in the forms of bubbles of gas migrating through the water-filled porous rock (Khilyuk et al., 2000). The mechanism of this type of migration is based on diffusion and buoyancy of the gas molecules which move from higher to lower gas concentrations (Liu et al., 2019). The discontinuous gas migration depends on porosity, permeability, and other rock properties rather than larger scale factors as the continuous gas migration (Ma et al. 2023).

The presence of gas in the shallow sediments in the Baltic Sea area was investigated in many studies using either seismic or hydro-acoustic data. Blanking and turbidity evidence of shallow gas was found in organic-rich near seafloor sediments in Arkona Basin (Mathys et al., 2005; Thießen et al., 2006) and in Eckernfoerde Bay (Abegg and Anderson, 1997; Huster et al., 2020). Shallow gas distribution in Holocene marine mud was mapped in Arhus Bay and Skagerrak (Jensen and Bennike, 2009; Laier and Jensen, 2007; Grob et al., 2020). Free gas in Holocene mud was also detected in the Bornholm Basin (Laier and Jensen, 2007; Tóth et al., 2014). Offshore Poland, studies on shallow gas were conducted since the early 90s (Jaśniewicz et al., 2019). The majority of the studies focused on the eastern and central part of the Polish Exclusive Economic Zone (EEZ), especially in the Gdansk Basin and the Słupsk Furrow (Jakacki et al., 2002; Tęgowski et al., 2003; Brodecka et al., 2013; Jørgensen and Fossing, 2012; Majewski and Klusek 2011, 2014; Idczak et al. 2020). Geochemical studies performed by the consortium led by the Polish Geological Institute in 2005-2008 indicated the occurrence of thermogenic gas in near seafloor waters (Jaworowski et al. 2010; Wagner, 2011). It was linked with the Paleozoic petroleum system, with active oil and gas production in the eastern part of the EEZ (Jaworowski et al. 2010). The area of Pomeranian Bight in the western part of the EEZ is less studied with the acoustic data collected during the 1970s and 1980s (Jaśniewicz et al., 2019).

In this study, we analyze multichannel reflection seismic (MCS), high-frequency hydro-acoustic (parametric sub-bottom profiler), and bathymetric (multibeam) data acquired in the greater Pomeranian Bight area, southern Baltic Sea. The study area is located at the offshore extension of the established Paleozoic (mostly Carboniferous) and Permian (both Zechstein and Rotliegend) petroleum play (Karnkowski et al., 2010). The shallow gas investigation were very limited in the offshore Pomerania compared to surrounding area such as the Eckernfoerde Bay, the Hano Bay, or the Gdansk basin due to the lack of data. The new comprehensive and multiscale dataset offers a unique opportunity to verify the above-mentioned observation of the potential geogenic gas leakage. Our data provide evidence for the gas presence in the shallow sediments, as well as its link with the deeper geological structure near the Trzebiatów Fault zone and the associated gas chimneys. Amplitude-versus-offset (AVO) analysis of seismic data confirms the presence of gas at the deeper reservoir level, while seismic data portrays gas migration pathways (gas chimneys).

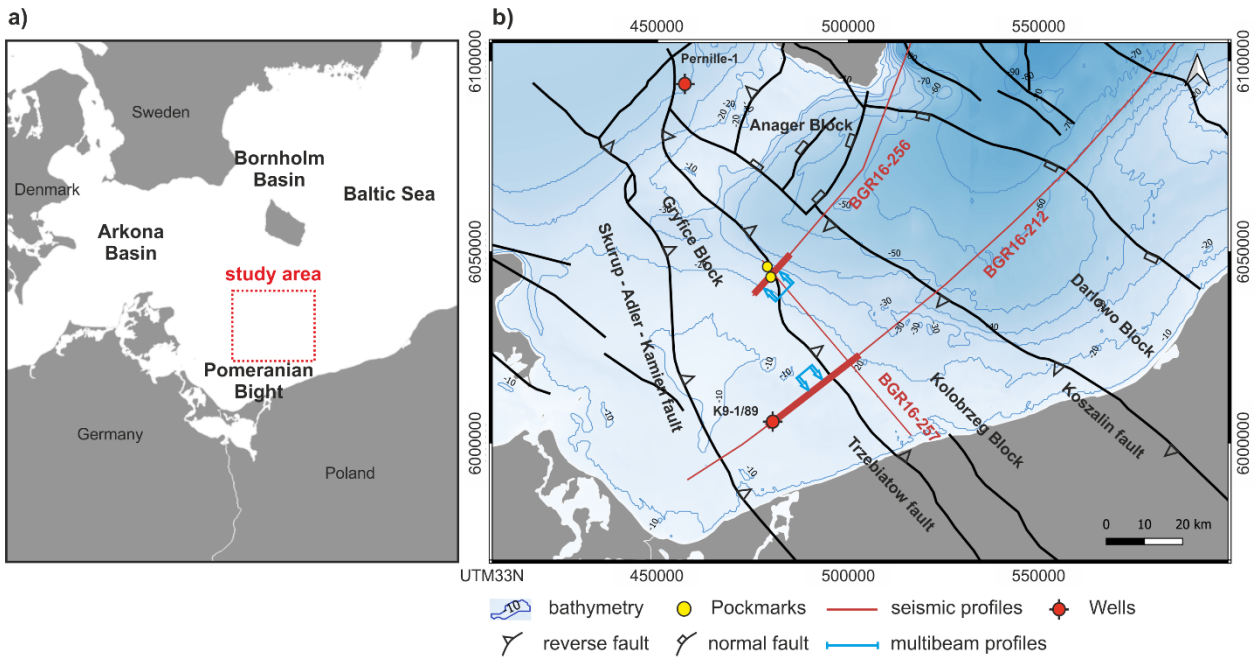

Figure 1. a) Location of the study area (greater Pomeranian Bight, Baltic Sea). b) Location of seismic lines used in this study on bathymetry map with main tectonic structures overlayed (modified from Janik et al., 2022). Part of the seismic lines showing shallow gas features are highlighted by a thick red line. Yellow dots show two pockmarks identified by multibeam data.

2. Geological background

The study area is located offshore Poland within area of Gryfice block, in the inverted part of the Permian - Mesozoic Polish Basin, so-called Mid - Polish Swell (Dadlez, 2003; Krzywiec, 2006). There are two main inversion-related fault zones: Adler-Kamień and Trzebiatów faults, rooted in the pre-Permian basement (Figure 1).

Development of the Permian - Mesozoic basin and its sediments distribution are consequences of two tectonic regimes: basin extension commenced in the Rotliegend through Mesozoic to Lower Cretaceous and later inversion tectonism in Late Cretaceous period (Vejbaek et al., 1994; Krzywiec, 2006, 2022). Dominant fault systems in the north western part of Mid-Polish Trough (MPT) are NW-SE trending (Scheck-Wenderoth and Lamarche, 2005). During extensional basin subsidence stage, sediments and structural features of the MPT were controlled by deep-seated and listric normal faults. These faults systems were then strongly reactivated in the basin inversion stage and extended from the basement upward into Mesozoic series (Vejbaek et al., 1994; Schlüter et al., 1997; Krzywiec, 2006), the Trzebiatów fault zone crossing our study area (Figure 1) is one of such faults. The Trzebiatów fault zone in the NE of the section

(Figure 3) is a typical extension fault system inverted in a compressional tectonic regime (Schlüter et al., 1997; Krzywiec, 2002), this fault zone roots within pre-Zechstein and accompanied by asymmetric fault-propagation folds developed within the Mesozoic sedimentation.

2.1. Sub-quaternary geology

Mesozoic sediments were studied by several authors (e.g., Dadlez, 1978, 1980, 2002, 2003; Krzywiec, 2006; Zimmermann et al., 2015) in this study area. Triassic sediments compose of red-bed sediments of fine grain sandstones, silt and shale in Lower and Upper Triassic whereas carbonate evaporates are dominant in Middle Triassic (Dadlez et al., 1995; Erlstrom et al., 1997). Potential seals in the petroleum play can be formed by thin claystones at the top of Keuper (Pernille-1 unpublished well report, 1989). Sediment deposits are consistent during Lower to Upper Jurassic with predominance of clay with interbedded interlaminated fine grain sand. Marine limestone is dominant lithology of the Upper Cretaceous to Early Paleogene. In this study, we consider the Upper Triassic succession as potential reservoir rocks (Figure 2, see section 2.3 below).

2.2. Quaternary geology

In the area of the Trzebiatów Fault zone offshore Poland, Tertiary sediments are almost absent due to erosion during Late Cretaceous - Paleogene inversion (Krzywiec, 2003, 2006), the Mesozoic formations are the direct substrate of the Quaternary sediments. The total thickness of the Quaternary formations in this region is estimated at about 30 - 40 m (Kramarska et al., 1999). The Quaternary profile in the south-eastern part of the Gryfice block is represented by the two levels of Pleistocene glacial tills, separated by a series of fluvio-glacial sands and gravels (Kramarska, 1998). The thickness of the lower till layer is estimated to be several meters, in some places it can reach about 10 m. The layer of the upper till is thinner, often topped with lacustrine sands, silts and gyttas, locally organic silts, and peat. These types of sediments can be found in many places in the Gryfice block. Numerous radiocarbon dates of organic sediments indicate that lake accumulation took place mainly in the early Holocene (e.g., Kramarska, 1998). The sea bottom surface is covered with a layer of fine-grained sands deposited in the Littorina and Post-Littorina sea, from the middle Holocene to the present day.

The Pleistocene sandy sediments are dominant in the north-western section of the Gryfice block. This sedimentary series lay directly on top of the older glacial till (the younger till is not present). The lower part of the sandy layer is most probably represented by fluvio-glacial sands and gravels. The upper part is a continuation of the fluvial and lacustrine sediments accumulated during the warming period MIS3 (interplenivistulian). The sediments identified in cores (Kramarska, 1998) are represented by sands and silty

sands with plant detritus and pieces of wood, dated with C14 at about 45-22 ka BP. The surficial part of the sand layer, with a thickness less than the resolution of the wave image, represents the marine environment of the younger Holocene.

2.3. Petroleum system of Western Pomerania

The petroleum system of Western Pomerania, encompassing both the onshore and offshore part of Poland extending to the eastern part of the Northeast German Basin, is specifically described in numerous studies (Karnkowski et al., 2010; Kotarba et al., 2004; Gawenda, 2011). Lithostratigraphic chart of petroleum system offshore Poland (Figure 2) is built based on nearby well stratigraphy data (Erlstrom et al., 1997; Pernille-1 unpublished well report, 1989). Source rocks in the Pomerania Bight are divided into two main units: the older Carboniferous deposits comprised of Tournaisian mudstones and claystones and the younger Zechstein Main Dolomite. Geochemical modeling of onshore Polish wells shows that both the Carboniferous source rock and Main Dolomite (Zechstein) display poor to fair source potential, and locally very good to excellent oil-source potential. The generation of hydrocarbons of both source rock types begins in the time span between the Middle Triassic and Late Jurassic (Kosakowski et al., 2006). Major recognized reservoir rocks are either Carboniferous or Rotliegend clastics, sealed by Zechstein evaporates (Karnkowski et al., 2010). Grainstones and packstones within the Main Dolomite (Zechstein) unit (Karnkowski et al., 2010) are forming the third reservoir level. Zechstein formation can be considered as a closed hydrocarbon play, where the source, reservoir and seal rocks are in the same location.

.

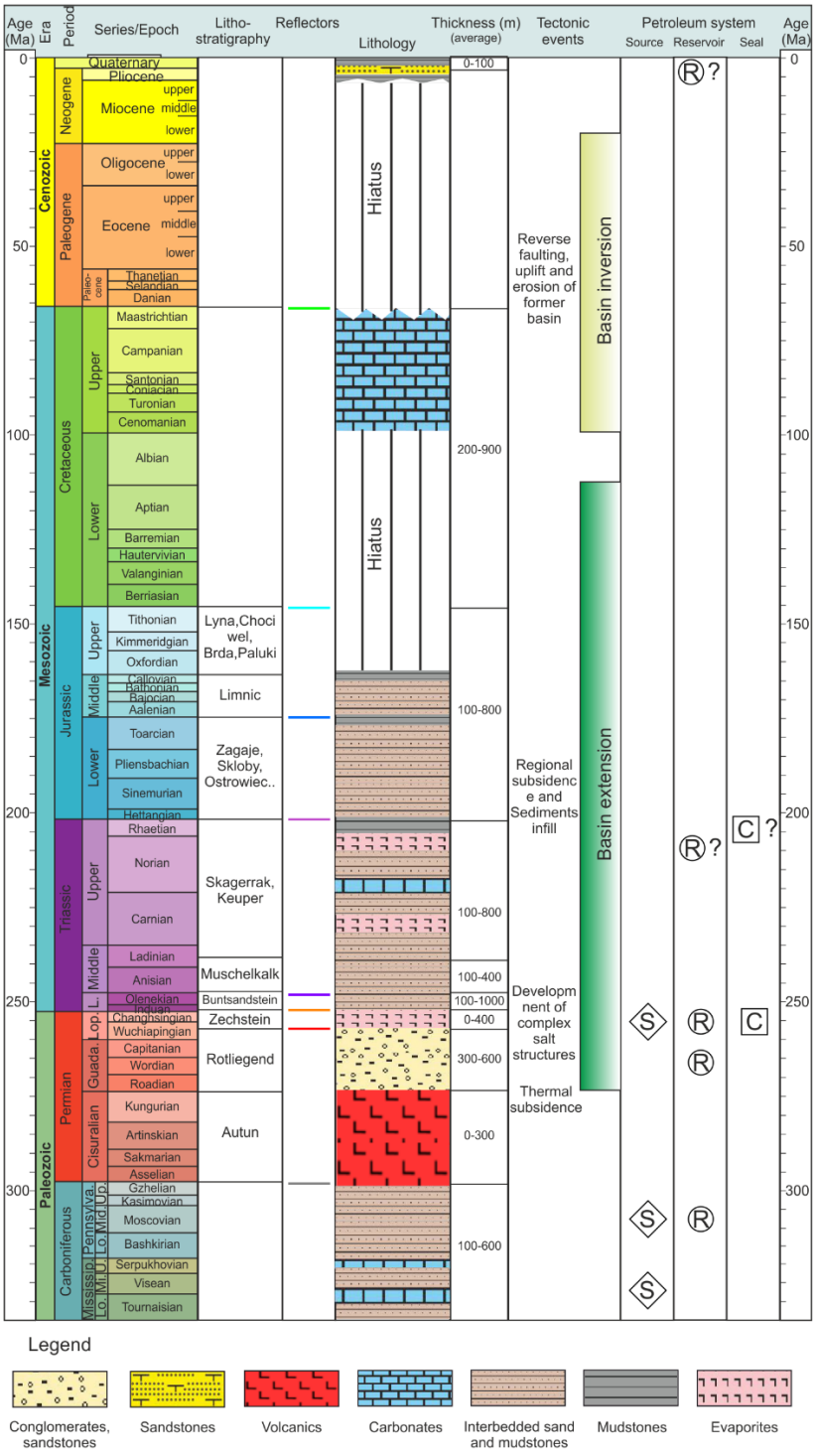

163

164 **Figure 2.** Simplified lithostratigraphy and petroleum system of West Pomeranian, offshore Poland. The
165 graph is based on well stratigraphy, tectonics, and lithology from Erlstrom et al. (1997) and Pernille-1
166 unpublished well report (1989).

3. Data and methods

Reflection seismic, hydro-acoustic and bathymetry data were acquired in March 2016 onboard R/V Maria S. Merian (see Hübscher et al., 2017). The cruise MSM52 collected ca. 3500 km of MCS data throughout large area from Bay of Kiel to north-east of Bornholm (Hübscher et al., 2017, Hübscher, 2018). This dataset allowed, e.g. to investigate the tectonic evolution of the Baltic Sea sector of the North German Basin (Ahlrichs et al., 2020, 2022, 2023), explain structural evolution and inversion tectonics along the Tornquist Zone (Krzywiec et al., 2022; Pan et al., 2022). Due to some malfunction of the parametric sediment profiler and multibeam echosounder, some of the seismic lines have no coverage of these data (see Table 1).

Data availability	**BGR16-212**	**BGR16-256**	**BGR16-257**
MCS	yes	yes	yes
Parametric sediment profiler	yes	yes	no
Multibeam	no	yes	yes
Shallow gas observations			
Gas chimneys	yes	yes	-
Pockmarks	-	yes	yes
Shallow geology			
Holocene mud	yes	no	no

Table 1. Data availability and shallow gas features in 3 profiles: BGR16-212, BGR16-256 and BGR16-257.

3.1. Multi-channel reflection seismic data and well data

MCS acquisition was tuned to provide high-resolution data and a gap-less image from the seafloor to deeper subsurface. Toward this end, relatively short minimum offset (37.5 m) and high-frequency air-gun array (8 GI guns) was employed. Acquisition parameters are summarized in Table 2.

Parameter	**Value**
Number of channels	216
Receiver group interval	12.5 m
Average shot interval	25 m
Minimum offset	37.5 m
Maximum offset	2710 m
Streamer tow depth	3 m

Airgun array tow depth	2 m
Airgun array	8 x GI guns (1200 inch^3 total volume)

Table 2. Acquisition parameters of MCS data acquired during the MSM52 cruise (Hübscher et al., 2017).

The MCS dataset was processed in-house at the Institute of Geophysics, Polish Academy of Sciences. Seismic data processing workflow included several demultiple techniques such as SRME, Tau-P deconvolution, and water bottom FK filtering (see more details in Nguyen, 2020 (processing report)). In this study, we use two profiles from MSM52 cruise (line BGR16-212 and BGR16-256) (see Figure 1 for location). Final seismic sections were pre-stack time migrated. The seismic reflectors were correlated with the stratigraphy horizons from nearby well K9-1/89, for which time-depth charts (check-shot data) and stratigraphy formation tops were provided (unpublished Petrobaltic report).

3.2. Hydro-acoustics data and bathymetry data

The uppermost sediment layers were surveyed using a parametric sediment profiler (PARASOUND DS III-P70 system) by simultaneously emitting two primary frequencies between 19 and 23.5 kHz, a parametric frequency of around 4 kHz is created, allowing for a maximum penetration depth of approximately 200 m beneath the seafloor, although in the area of shallow water, the image recorded was clear for interpretation up to a dozen of meters beneath the seafloor (above the multiple). The hydro-acoustics data were processed using MDPS (Meridata, Finland) software.

The seafloor morphology was surveyed by a hull-mounted SIMRAD EM122 multibeam echo-sounder system. Multibeam data were processed using QINSY and QIMERA software. The raw data files have been loaded into QIMERA as Processed Point files (QPD). The processing used a strong spline filter and CUBE processing. In addition, due to the lack of repeated water sound velocity profiles, external beams were rejected and refraction correction was added. Bathymetry grids with regular 0.75 m cells were created for the analyzed profiles. The multibeam data lateral resolution was between 0,5-1,0 m. The vertical measurement accuracy was +/- 12 cm.

3.3. Seismic attributes and amplitude versus offset analysis

Seismic attributes are commonly used in seismic interpretation to automate highlighting specific features, often difficult to decipher by human interpreters (Marfurt, 2018). Seismic attributes can help in tracking fluid expulsion (e.g., gas escape features) (Cartwright and Santamarina, 2015) and dissolution or collapse features (e.g., Sullivan et al., 2006; Singh et al., 2016; Meldahl et al.,1999). So-called geometrical attributes (Chopra and Marfurt, 2007), such as the coherence attribute, are commonly used in the detection of faults,

fractures, and chaotic zones. The coherence seismic attribute seems to be an effective tool to lineate free gas-associated features from other seismic events in the section. Due to the absorption and scattering of the seismic energy, the chaotic behavior of the seismic signal of the gas chimneys and acoustic blanking can be differentiated compared to continuous seismic events of adjacent areas within the section.

Amplitude versus offset (AVO) can be considered as a specific quantitative seismic interpretation attribute. It is commonly used in the oil and gas exploration industry to identify reservoir zones, fluids, and lithologies. The two AVO attributes, AVO Intercept and Gradient, are calculated from pre-stack angle gathers using Aki-Richards 2-term equation (Aki and Richards, 1980), an approximation of full Zoeppritz reflectivity equations (Hilterman, 2001). Intercept is the P-wave reflection coefficient at the normal incidence of an event, while gradient represents a regression of amplitude variations taken at different angles of incidence (Russell, 2002). AVO technique is rarely applied in shallow gas studies because of problems in obtaining sufficient angle coverage at shallow depths, however, it can be used to check where the gas distribution on the seismic section and where the gas can migrate to the seafloor.

In order to prove the existence of free gas remnants in the potential reservoir and to discriminate fluid effect with normal background rock property, we performed AVO analysis. We followed a conventional workflow of AVO application. First, the CDP gathers are muted to remove traces beyond the maximum incident angle of 45 degrees (angle mute). The signal-to-noise ratio is improved through super gather creation and residual move-out is eliminated through trim statics.

4. Results

4.1. Line BGR16 – 212

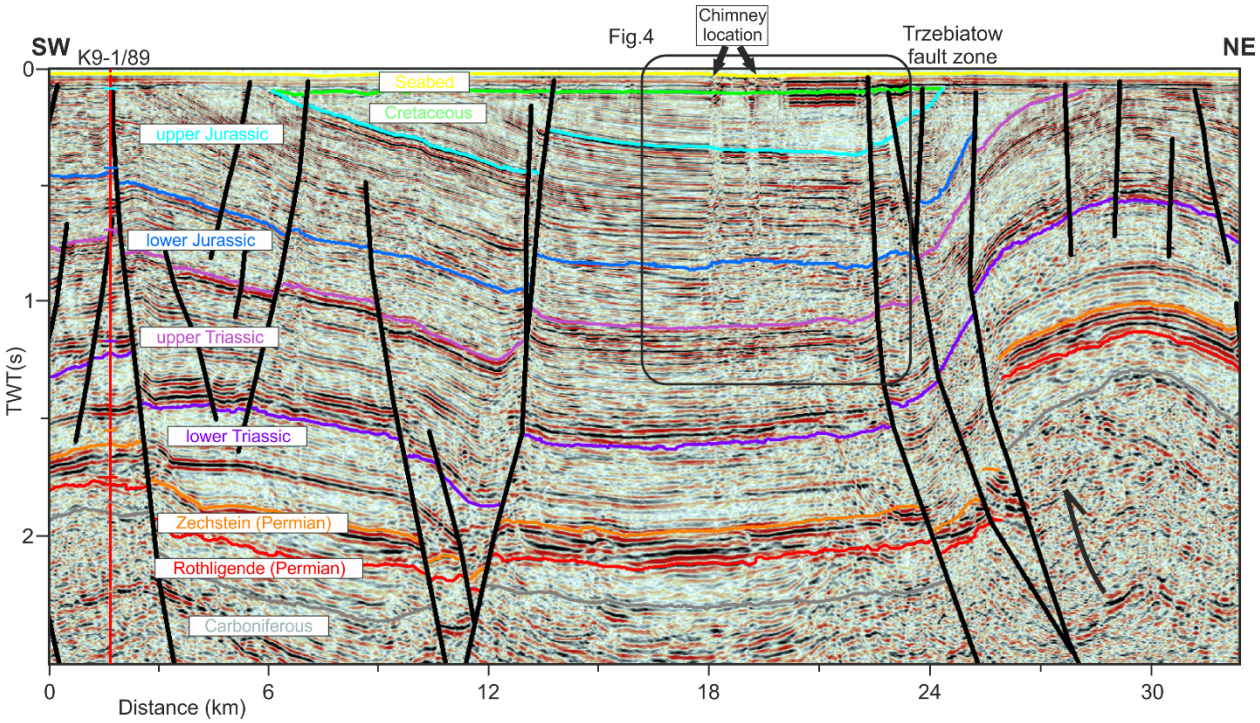

229

230 **Figure 3.** Part of the interpreted pre-stack time migrated seismic section along profile BGR16-212 across
231 well K9-1/89, the Trzebiatów fault zone and the Gryfice block (see Figure 1 for the location of the seismic
232 profile and well). Two gas chimneys were identified near the eastern part of the Gryfice block, close to the
233 Trzebiatów fault zone. The rectangle marks the area displayed in Figure 4.

234 Line BGR16-212 crosses important geological features such as Adler-Kamien and Trzebiatów faults zone
235 (Figure 3). Interpretation was based on well K9-1/89 stratigraphy markers, unpublished well reports,
236 regional cross sections and previous studies (both offshore and onshore) (Jaworowski et al., 2010; Pokorski,
237 2010; Krzywiec, 2006). Line BGR16-212 shows an asymmetric fault-propagation fold accompanied by a
238 reverse Trzebiatów fault zone in the NE of the section (Figure 3). Toward the SW of the section, there are
239 few normal faults systems formed during the syn-rift basin extensional period. Sediment thicknesses of the
240 Mesozoic remain stable in this area. Notice that the Cretaceous formation is significantly eroded due to
241 strong uplift of inversion anticlines, only a small amount of 100-300 ms of Upper Cretaceous sediment was
242 left over in the Gryfice block (Figure 3). Two gas chimneys are identified in the section (Figure 4) together
243 with the high amplitude reflections (bright spots) close to the Trzebiatów fault zone.

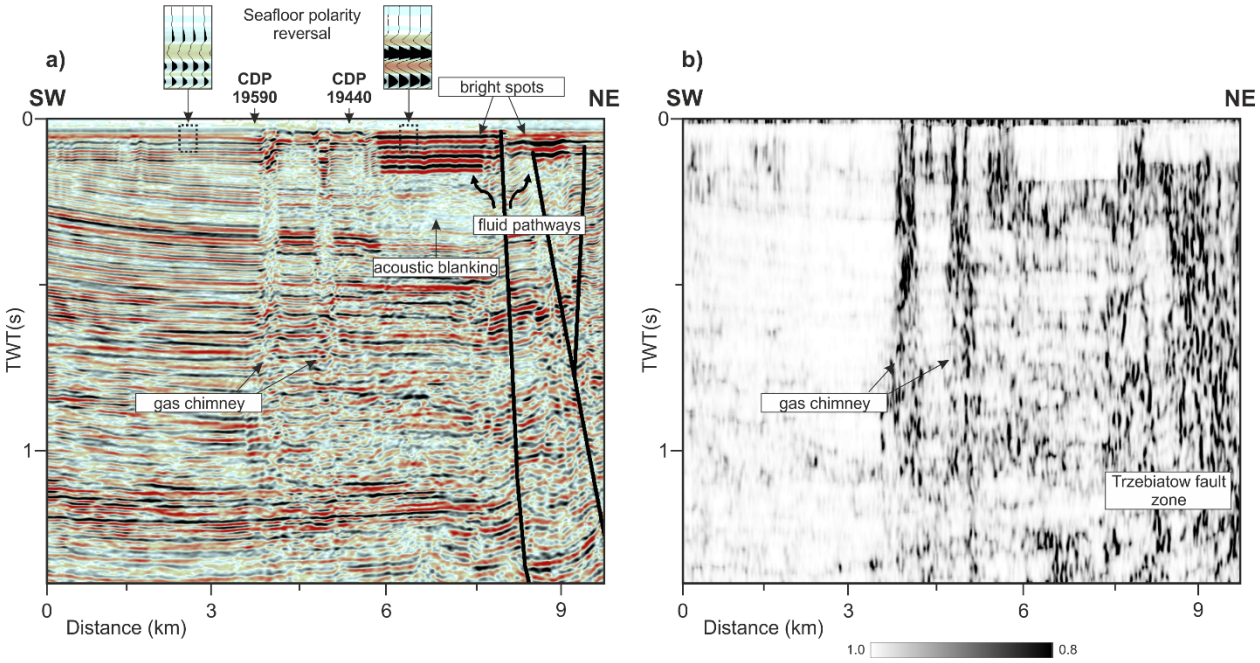

Figure 4. Part of the seismic section BGR16-212 (a) and its coherence attribute section (b). Evidence of shallow gas features is interpreted including gas chimneys, bright spots (enhanced reflection), acoustic blanking and seafloor polarity reversal.

Zoom in part of section BGR16-212 provides a clearer image of the shallow gas features (Figure 4). The reflectivity of gas chimneys appears as a chaotic zone, with low trace-to-trace coherence and lower amplitudes as compared with adjacent sediments. The coherence seismic attribute was employed to help interpret free gas-associated features (Figure 4b). Gas chimneys are more discriminated as high coherence values to continuous events. The Trzebiatów fault zone is also highlighted as a noisy area due to discontinuous reflectivity at the fault location. More importantly, low coherence zone of the gas columns is much reduced around intervals of 1.1 to 1.2 s, which may suggest the potential existence of a gas reservoir in the past at this interval.

Apart from polarity reversal, bright spots, and gas chimneys, the acoustic blanking zone is identified below the bright spots and reverberations in the seismic section (Figure 4a). In this case, acoustic blanking happened below the bright spots, which indicates attenuation of seismic energy by the gas-charged sediments.

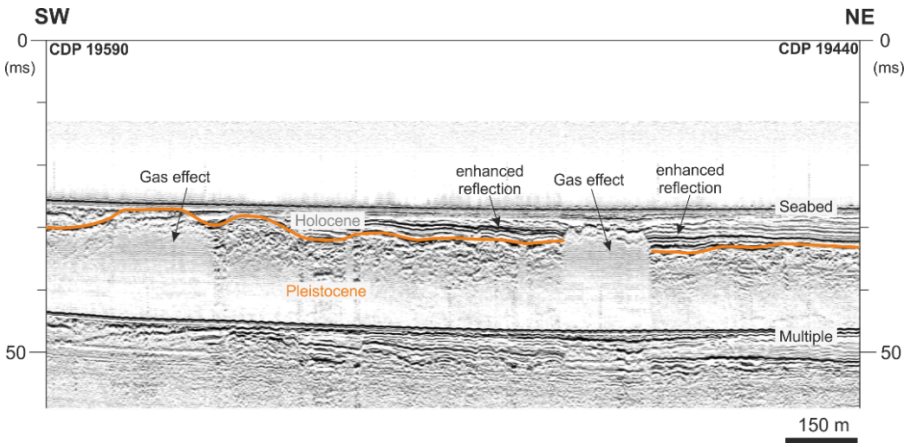

Figure 5. Hydro-acoustic data (parametric sediment profiler) from profile BGR16-212 between CDP 19440 to 19590, crossing gas chimneys identified in the MCS data. The boundary between Pleistocene and Holocene sediments (orange) is interpreted in this profile.

The gas chimneys identified in seismic data are also associated with disturbances in amplitude patterns in the parametric sounding data (Figure 5). Gas chimneys are clearly marked within the Pleistocene sediments as non-reflective vertical zones. The width of the two zones identified along the profile is approximately 150 and 250 m, respectively. Chimneys/anomalous amplitude zones do not reach the sea bottom - the gas reaches the upper glacial till or is dispersed in the paleolakes' sediment layer. Close to the gas effect zones, some enhanced reflections are identified (Figure 5), which may prove that the gas is charged to Holocene sediments instead of leaking to the seafloor. However, such reflections may also result from the lithological variability (e.g. presence of organic layers, such as pit, gytta) or/and deposits structure (e.g., layering/stratification).

4.2. Line BGR16 – 256

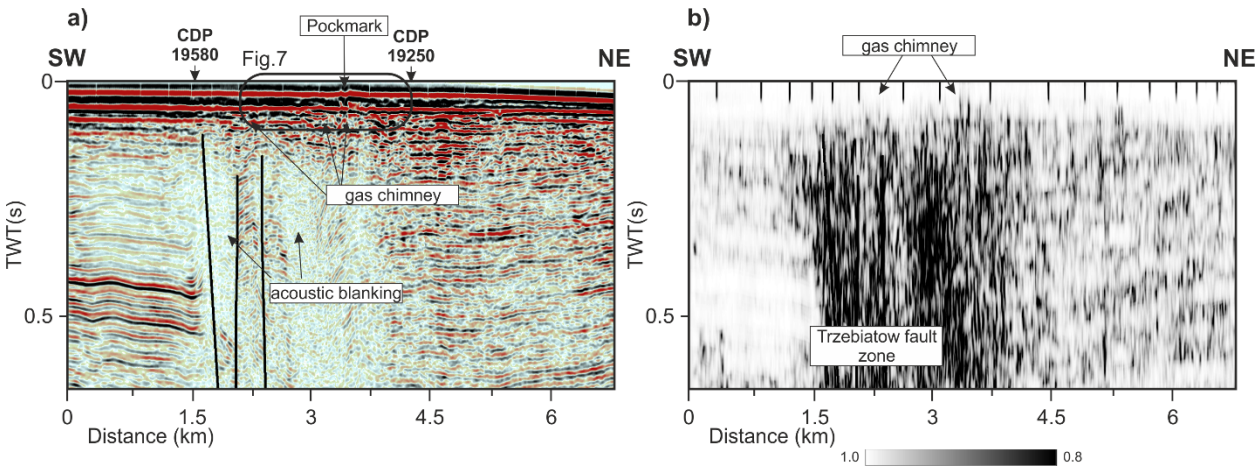

274

275 **Figure 6.** Part of the pre-stack time migrated seismic section along profile BGR16-256 and the
276 corresponding coherence attribute section (see Figure 1 for the location of the seismic profile). Evidence of
277 shallow gas features is interpreted including gas chimneys, acoustic blanking, and pockmarks.

278 Shallow gas expressions were also interpreted along profile BGR16-256 toward the northwest of the
279 Trzebiatów fault zone. We identified gas chimneys, acoustic blanking, and pockmarks in the seismic section
280 (Figure 6). The columns of gas are much smaller than observed along line BGR16-212. They may only be
281 recognized by little polarity changes close to the seafloor (Figure 7). The utility of the coherence attribute
282 section is minimal in this case as the locations of these gas columns are close to the complicated Trzebiatów
283 fault zone. Acoustic blanking zones in this line appear at around 0.2 to 0.5 s joint with the fault zone (Figure
284 6). The coherence attribute shows a large low-value zone which represents a huge discontinuity zone due
285 to faulting, fracturing, and presumed free gas activities.

286 The analysis of the bathymetric data along lines BGR16-256 and BGR16-257 (seismic data from the latter
287 were not interpreted as it follows the strike of the Trzebiatów fault) indicates that in some places the gas
288 also reaches the seafloor, creating small oval depressions (Figure 7). The asymmetric form recorded along
289 line BGR16-256 is about 35 m in diameter and 0.6 m deep (Figure 7a). Features identified along line
290 BGR16-257 are smaller, approximately 25 m in diameter, and only 0.2 m deep (Figure 7b).

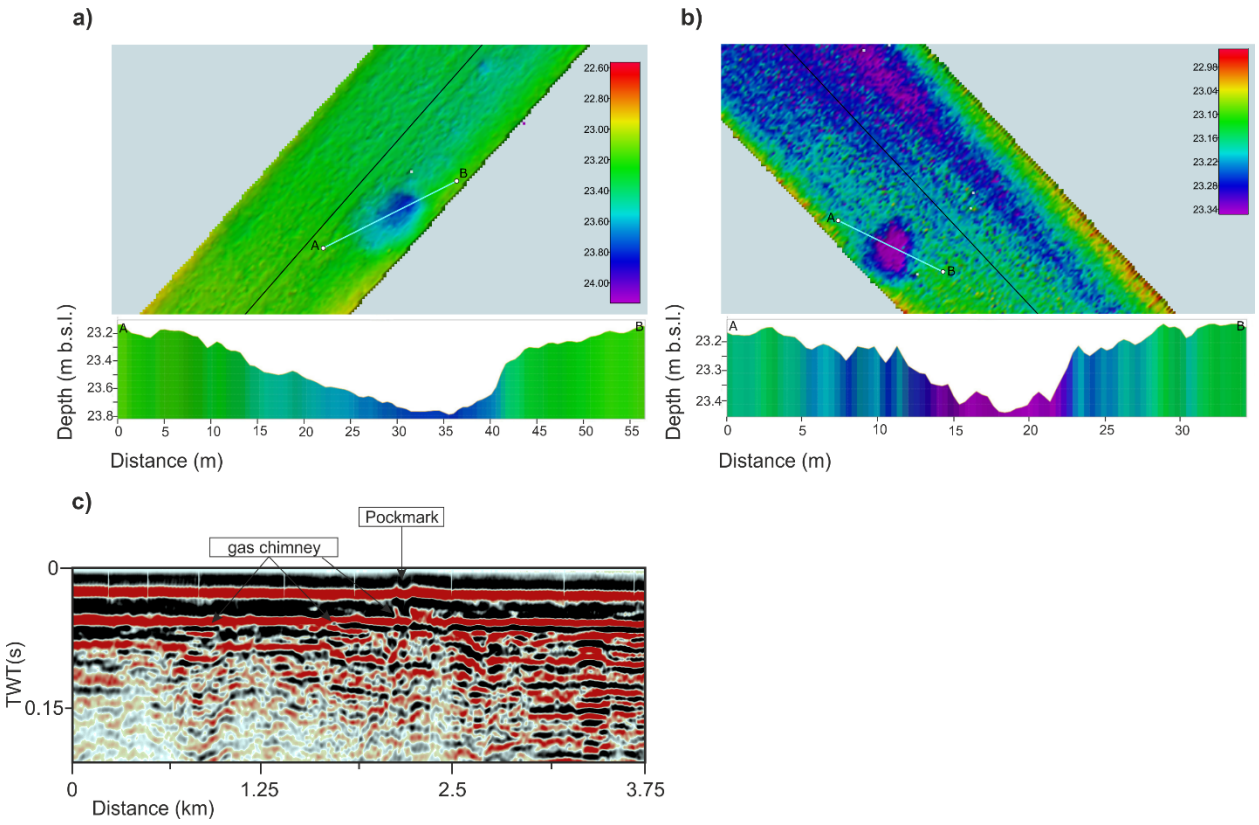

Figure 7. Seafloor topography build from multibeam data close to the pockmark identified along line BGR16-256 (a). Seafloor expressions of a pockmark identified at the strike profile (BGR16-257) (b). For position of these pockmarks, see Figure 1. (c) Part of the seismic section profile BGR16-256 at the identified pockmark location.

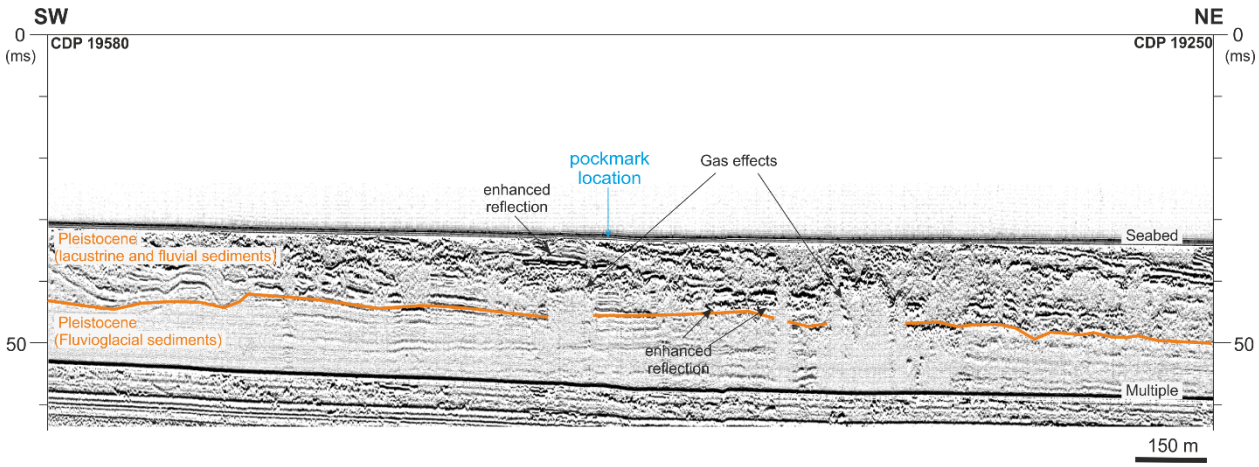

Figure 8. Hydro-acoustic data (parametric sediment profiler) from profile BGR16-256 between CDP 19250 and 19580, crossing the gas chimneys and pockmark in line BGR16-256. The boundary between 2 types of

Pleistocene sediments (orange) is interpreted whereas Holocene mud sediment is absent in this profile. Note that the pockmark is not recognized in this hydro-acoustic data.

Gas chimneys are less pronounced in the parametric sediment profiler data (Figure 8) than in line BGR16-212. It is possible that in an environment with a distinct predominance of non-cohesive deposits, represented here by fluvial and lacustrine sands and silty sands of MIS3, the gas is more easily dispersed inside the layers of these deposits. Anomalies caused by gas columns are still recognizable. Enhanced reflection zones, identified surrounding these anomalies probably indicate the occurrence of more cohesive inter-layers, hardly permeable to gas. The structure of these layers is variable and locally the gas reaches the seafloor forming small pockmarks (Figure 7). Toward the SW part, the hydro-acoustic data become significantly lower quality (Figure 8). It can be also caused by shallow gas activity.

4.3. AVO analysis along line BGR16-212

AVO analysis is carried out at the presumed location of the potential gas accumulation within the Upper Triassic formation (root zone of gas chimneys identified along line BGR16-212, Figure 4). The target zone of AVO analysis is restricted at the interval of 100 ms (around 1.1 to 1.2 s TWT) and limited between the Trzebiatów Fault and a normal fault in the SW of the section. Figure 9 shows 3 angle gathers at selected locations surrounding the gas chimneys (CDP numbers 19420, 19640, and 19750) (see the location of the CDP gathers in Figure 10). Notice that the three CDP gathers were chosen based on scanning through the whole NMO-corrected CDP gathers of line BGR16-212 as most representative CDP gathers exhibiting AVO effect at the interesting interval.

The CDP gathers were corrected using processing velocity. The top horizon (red) is marked at ~1.11 s as the top of the reservoir. The bottom horizon (green) is marked at ~1.21 s as a presumed base of the reservoir (Figure 9). The top and base of the potential reservoir here were based on enhanced reflections visible in the seismic section. They may not represent for true top and base of the gas deposit in the potential reservoir. The AVO Intercept and AVO Gradient were selected from the major trough and peak pair at 3 CDPs (19420, 19640, and 19750) (Figure 10). The amplitude variation clearly shows class 2 AVO which has a small negative reflection coefficient at zero offset and amplitude increase with offset (Castagna and Swan, 1997) in 3 CDP gathers. This trend indicates the presence of remnant free gas in the Upper Triassic reservoir rocks.

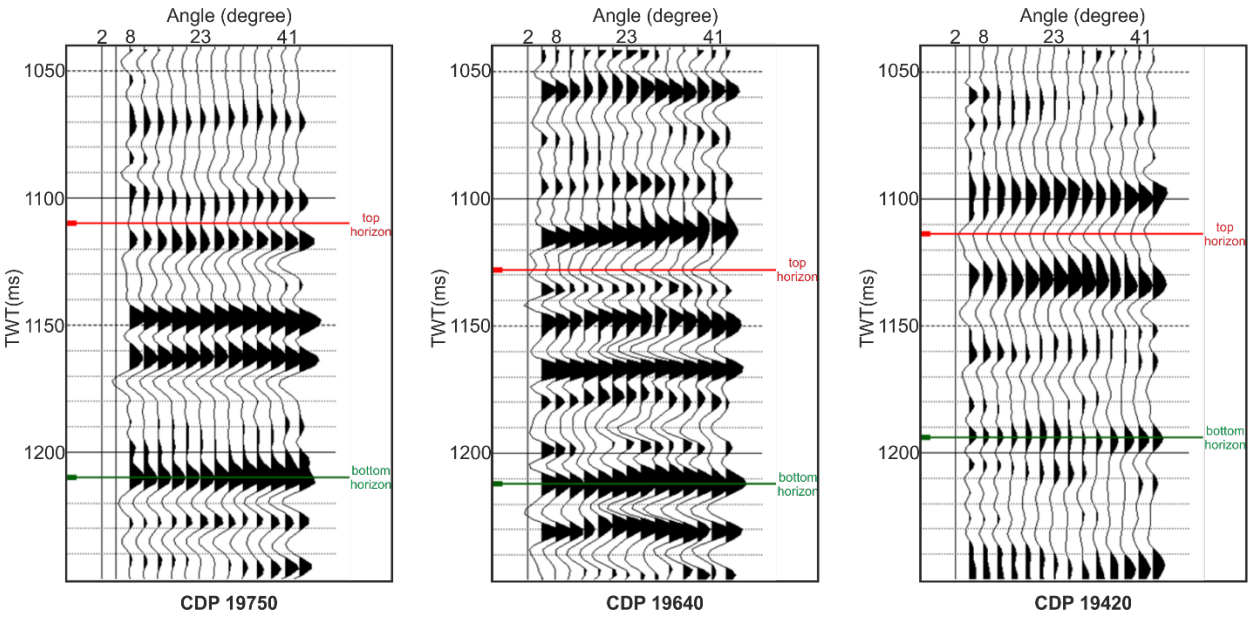

Figure 9. Angle gather extracted from profile BGR16-212, at CDP super gathers 19750, 19640 and 19420. Locations of the CDP points on the stack section are shown in Figure 10. The top horizon (red) marks top of the potential reservoir, the bottom horizon marks base of the potential reservoir. Normal move-out correction is applied using stacking velocity.

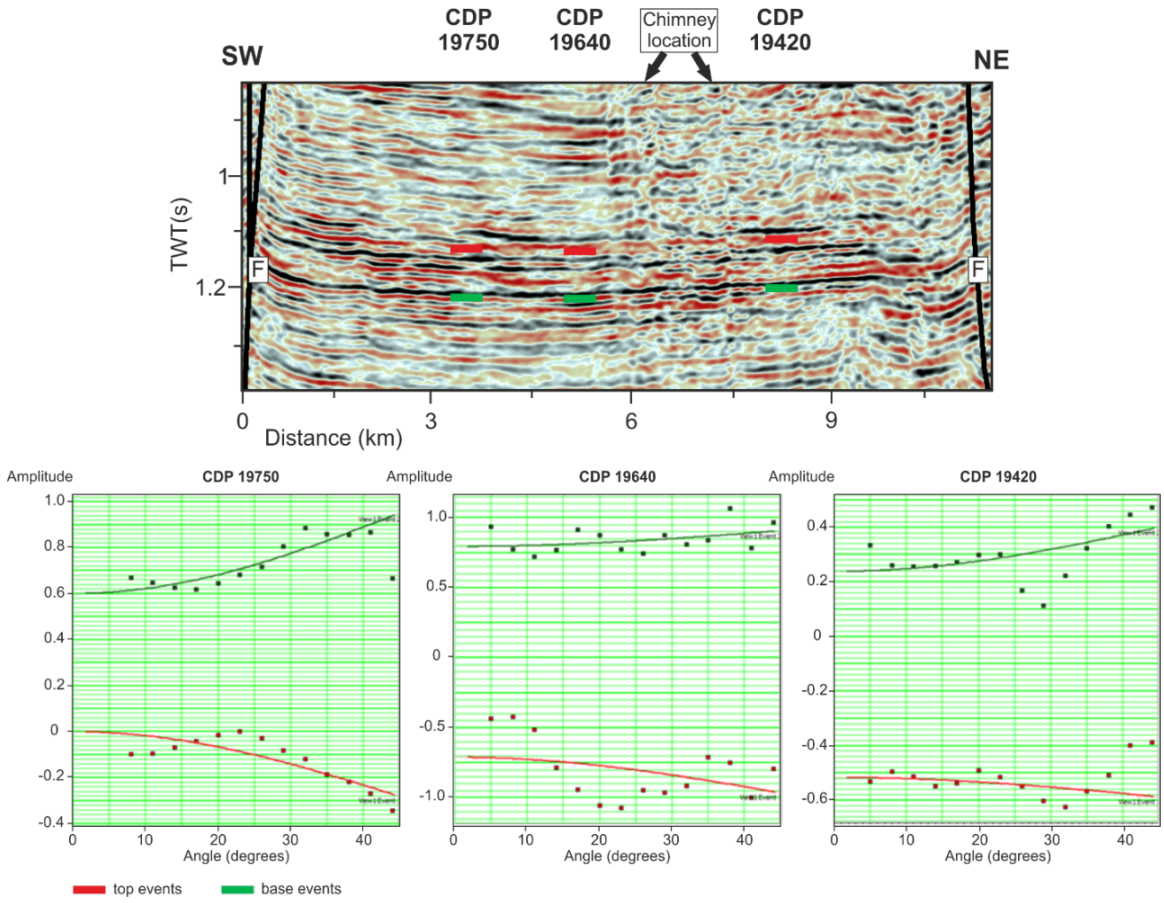

Figure 10. Gradient analysis of the angle gathers shown in Figure 9. Locations of the CDP gathers are chosen surrounding the chimneys' locations and at the potential reservoir interval (a). (b) Trough (red) and peak (green) seismic amplitudes are displayed with angle (offsets) at the depth of around 1.15 s TWT for CDP numbers 19420, 19640, and 19750.

Cross-plot of the derived AVO Intercept/Gradient is presented in Figure 11 to further investigate the type of AVO anomalies. The expected background trend is delineated as zone 1, while anomalous events were delineated as zone 2, consistent with class 2 AVO anomalies. Both zones were projected back onto the seismic section. AVO anomalies interpreted as free gas-charged sediments (red color) are highlighted in the section (Figure 11). The majority of the free gas-related anomalies are located within the predicted potential gas reservoir and along the gas chimneys' pathways.

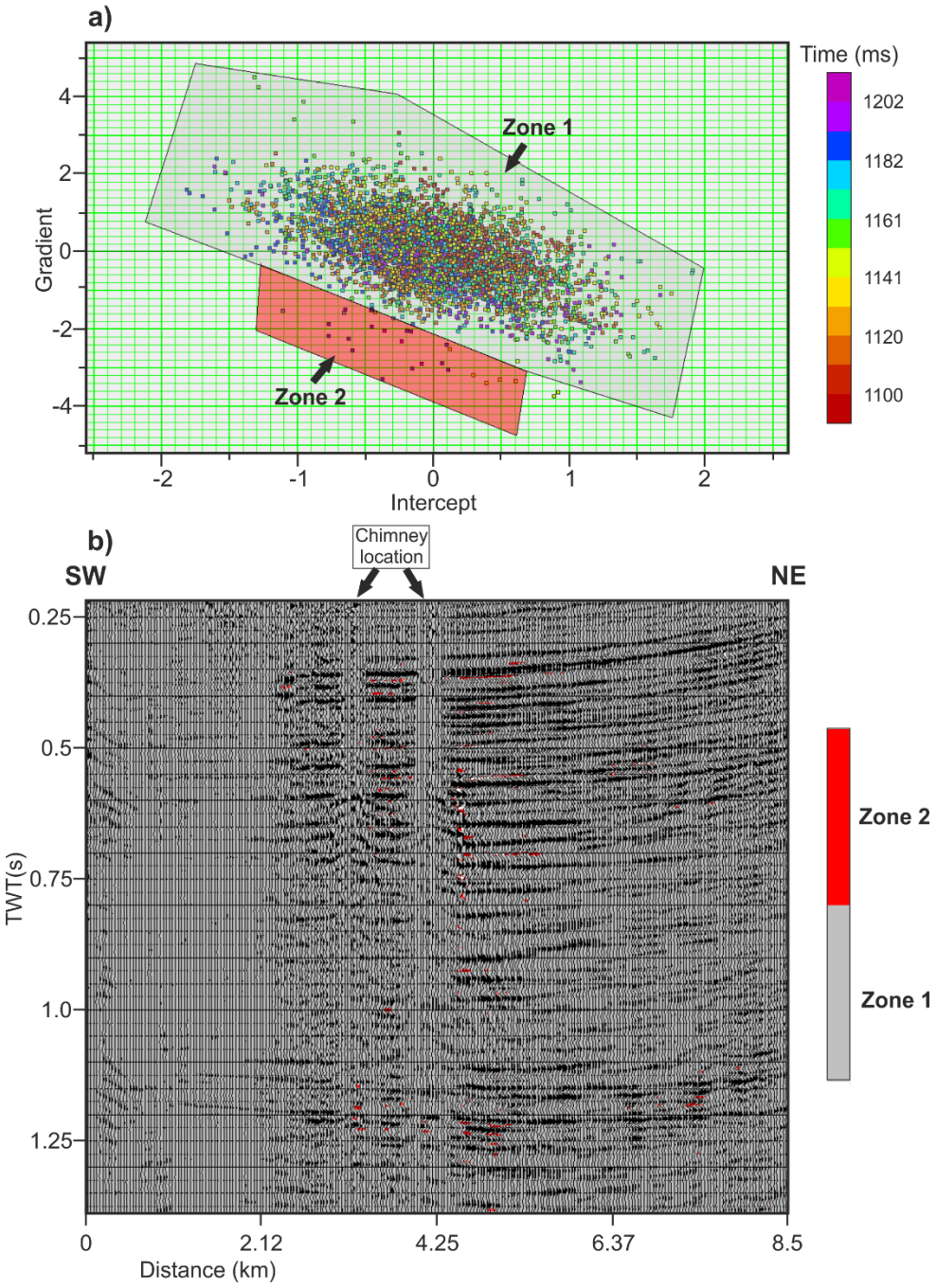

Figure 11. AVO Intercept/Gradient cross-plot and seismic amplitude and AVO anomaly section along part of line BGR16-212. (a) Cross-plot shows the background trend (grey) (zone 1) and AVO anomaly (red) (zone 2). (b) Zone 1 and 2 are mapped on seismic sections close to the chimneys' location.

5. Discussion

5.1. Seismic and hydro-acoustic indicators of shallow gas

5.1.1. Gas effects by seismic profiles

Evidence of the free gas in sediments of the Gryfice block is proved by indicative shallow gas features including gas chimneys, seafloor polarity reversal, bright spots, acoustic blanking, and pockmarks. Two big gas chimneys interpreted along line BGR16-212 can be tracked down with the support of seismic attributes to around 1.1 - 1.2 s TWT. This suggests the rooting of these gas chimneys at the Upper Triassic formation. The gas chimneys identified in line BGR16-256 (Figure 6) are less distinct and behave more as seepage style, which is "small and localized" (Schroot and Schuttenhelm, 2003; Spatola et al.,2018). These small gas seepages possibly leak slowly to the seafloor through tiny holes or gaps caused by faults' activities. Such structures are visible closer to the Trzebiatów fault zone, indicating an escape path of the free gas from deeper successions to shallow sediments. The free gas possibly begins to migrate during the Late Cretaceous inversion period together with the inverted activity of the Trzebiatów fault zone. Gas reaches also Pleistocene and Holocene deposits. Leaking of the gas associated with the pockmarks was registered close to lines BGR16-256/257 (no multibeam data available for line BGR16-212).

Bright spots identified on top of the Trzebiatów fault zone (Figure 4a), suggesting a potential of free gas migration pathway through the faults to shallow sediments. Amplitudes of these bright reflection shown as peak (positive) withreverse polarity to the seafloor reflection (Figure 4a). Bright spot areas are associated with the reverberations, as the consequence of strong impedance contrast between the layers of gas accumulated in shallow sediments (Davy, 1992; Tóth et al., 2014). It is impossible to differentiate these reverberations with the main reflector due to the very shallow water environment of the Baltic Sea (~30 ms in this area).

The attribute section enabled to delineate the rooting point of the gas chimneys along line BGR16-212 (Figure 4). The attribute anomalies of the columns start from around 1.2 s TWT. It suggests an upward pathway for the free gas to migrate from the Upper Triassic formation to shallow formations. The Trzebiatów fault zone appears as a mixture of coherence anomalies due to the discontinuity of seismic events within a complex faults zone. For profile BGR16-256 (Figure 6), the anomalies caused by gas or faulting are difficult to be differentiated as the location of small gas chimneys is too close to the Trzebiatów fault zone. However, this may prove that the gas migrates from much deeper to shallow sediments and then to the surface through the faults system.

Apart from indicated gas features, velocity pull-down is a typical feature represented for free gas presence in sediments underneath the seafloor. It happens because the compressional wave propagation velocity is decreased below the value for water-saturated sediment, attenuation of acoustic waves propagating through gassy sediment, and acoustic reflection and/or scattering are increased (Anderson and Bryant, 1990). The

problem of imaging artifacts in form of pull-downs is contrasted with the pull-ups concept caused by high-velocity localized anomaly (e.g., till within tunnel valleys; Frahm et al., 2020). Geological structures below the gas-charged shallow sediments could be misinterpreted as localized syncline-like features. Some of these features are visible in the gas chimney area in line BGR16-212 (Figure 4), however the far- and near-offset stacks, as well as the general appearance of the reflectivity inside the chimney, suggest that it is not caused by the dimming of the reflections due to the shallow gas anomaly only. What we observe in the seismic data is probably a combination of those two effects: shallow low-velocity anomaly and extensive fluid (gas) escape route.

5.1.2. Gas effects by acoustic profiles

This acoustic blanking below the gas-charged layers (Figure 5) represents low reflection and interruption image of the below sediment layer due to the presence of free gas (Tóth et al., 2014). It also appears that the gas columns did not reach the water bottom and stopped within Holocene/Pleistocene sediments boundary. It is possible that after migrating from the below successions, the free gas did not escape through the seafloor but might accumulate to very shallow sediments (Pleistocene – early Holocene). This hypothesis is further reinforced by the presence of bright spots close to the gas columns as well as polarity reversals of the seafloor reflectors. Besides, in the seismic section, these high-amplitude reflectors cause heavy reverberations below the water bottom (Toth et al., 2014). Enhanced reflection in layers deposited within the Holocene formation may indicate the occurrence of more cohesive, hardly permeable to gas internal layers, where the gas accumulates. This parasound image is similar to gas accumulation structures in Holocene marine mud that were recorded in the Bay of Aarhus (Jensen and Bennike, 2009), Bornholm Basin (Laier and Jensen, 2007; Tóth et al., 2014) and other sedimentation basins of the Southern Baltic Sea (e.g., Jaśniewicz et al., 2019; Idczak, et al., 2020).

Gas effects are more recognized along line BGR16-256 (Figure 8), which most probably result from different lithological formations of Quaternary deposits in this area (Kramarska, 1998). Two types of Pleistocene sediments can be differentiated by amplitude, chaotic reflection of lacustrine and fluvial origins sediments, compared to the dim and flat reflection of fluvio-glacial origin sediments. Seismic anomalies caused by gas activities can be identified by scattering points and blanking zones within the fluvio-glacial related sands and fluvial and lacustrine related fine-grained sands. These sands could possibly be potential deposits of the free gas in Pleistocene sediments. The pockmarks identified by multibeam data (Figure 7) and enhanced reflection features identified surrounding the gas effects illustrate simultaneous free gas accumulation and seafloor leakage (Micallef et al., 2019).

.

5.2. AVO attribute analysis

After interpreting the indicators of shallow gas in the seismic section, a starting point of the gas chimneys in line BGR16-212 is recognized by the coherence seismic attributes. It reveals a possibility of a potential gas reservoir existence at around 1.1 to 1.2 s TWT, in the Upper Triassic formation, so there is a high chance there are still free gas remains in this interval. Due to limited of lithology information and lack of well data, to verify this hypothesis, AVO analysis was only used to detect the remnant of free gas in the potential reservoir.

Accumulation of gas in sediments causes a decrease in velocity and density, therefore there will be a decrease in acoustic impedance (AI) of the formation (Simm and Bacon, 2014). The angle gathers from line BGR16-212 shows the increase of amplitudes in far offsets which represents for the decrease of AI due to free gas presence (Figure 9). AVO class 2 anomalies from the angle gathers were identified by gradient analysis plots as near zero impedance contrast between charged gas sand and surrounding non-gas sand and shale (mudstones). The class 2 AVO illustrates the similar properties of mudstones and gas sands at the presumed reservoirs interval and nature of the sand is compacted and cemented. This matches with lithology of the Triassic and Jurassic formations in the Gryfice block dominantly composing of interbedded sands and mudstones with very thin carbonate and evaporates layers (Figure 2). It might be concluded that the free gas could not be trapped permanently at the potential reservoirs due to lithology similarity between Mesozoic sediments and absence of good overlying seal.

In the scatter plot of intercept against gradient (Figure 11a), the low negative gradient represents for contained gas rock (zone 2, red) was discriminated from the background trend of surrounding normal rock property (zone 1, grey). Therefore, samples with no AVO behavior in grey polygon (zone 1) could imply for this dominant interbedded sand and mudstones, while it is not possible to conclude precisely the type of sand that contains the free gas in red zone (zone 2) due to lack of nearby well data information. So in this study, we just call it gas-charged sand. The free gas was exactly highlighted in the section, not only at the potential reservoir interval (1.1 – 1.2 s TWT) but also in whole Upper Triassic – Jurassic formation. Free gas distribution in seismic section (Figure 11) proves the hypothesis of origin of the gas chimneys and free gas “crept” to sediment layers throughout the gas chimneys migration pathways.

AVO technique was rarely applied in other fields than petroleum exploration, especially for shallow gas study. Kim et al., (2020) was possibly the only study that included AVO analysis for identifying free gas, helping to discriminate water contacts and bright events among the chaotic signals on the MCS data.

5.3. Petroleum system and shallow gas expressions

Linking of shallow gas to near seafloor sediments was carried out in several investigations in nearby areas of the offshore West Pomerania, southern Baltic Sea. Connections of geological settings of near seafloor sediments with distribution of methane were shown in Eckernförde Bay (Abegg and Anderson, 1997) and in Aarhus Bay (Jensen and Bennike, 2009). In Arkona Basin, characterization of acoustic turbidity caused by gas presence in near seafloor sediments were investigated by geochemical, core analysis, and very high-resolution seismic profiles (Mathys et al. 2005, Thieben et al. 2006). In Bornholm Basin, Tóth et al. (2014) linked free shallow gas with organic-rich Holocene marine mud by velocity field analysis in MCS data. Further north and east of Gotland Basin, Schäfer et al. (2021) interpreted phase-reversed seismic reflections beneath the Quaternary Klints Bank drumlin as evidence for hydrocarbon gas accumulation of thermogenic origin.

In this study, the shallow gas expressions from seismic and hydroacoustic data illustrate a leaking hydrocarbon play offshore West Pomerania. The free gas probably generates initially from the source rocks in Palaeozoic and Permian (Carboniferous mudstones and Main Dolomite Zechstein) (Kotarba et al., 2008; Karnkowski et al., 2010). The free gas then escapes to upper sediments through either the Trzebiatów fault zone or directly in areas where the Zechstein evaporates are thin or absent. This is more likely to happen when dominant sediments of Lower to Middle Triassic compose of just interbedded sand and mudstones layers. The Keuper (Middle - Upper Triassic) formation comprises of various types of potential reservoir rocks: fine grain sandstone and carbonate evaporates. In addition, the oil and gas prone window of the West Pomeranian falls into this period (Kosakowski et al., 2006; Karnkowski et al., 2010). Therefore, there are favorable conditions that the free gas can charge these rocks. Moreover, AVO analysis at the potential reservoir interval also proves the presence of remnant free gas in the Upper Triassic formation.

Based on the seismic interpretation, seismic attributes, and lithology of the study area, there are two possible migration pathways of free gas from the potential reservoir in the Upper Triassic sediments to the seafloor: through gas chimneys and through reactivated (during Late Cretaceous inversion) Trzebiatów fault zone. The first migration pathway might be explained that there is inefficient seal layer on top of the Upper Triassic formation, and free gas could migrate through unconsolidated successions above to the near seafloor. The second migration pathway might be due to strong reactivation of the existing listric faults, which created spaces for free gas to escape to the shallow sediments.

Evidence for geogenic pollution of Baltic Sea sediments along the Trzebiatów Fault has been provided by Jaworoski et al. (2010). As summarized by Wagner (2011), liquid hydrocarbon seepage into bottom waters results in maximum values of 96–193 mg/l, hence representing a considerable pollution of natural environment. The content of methane in waters is high in the southern part of the fault zone is up to 10.5–

60.1 ×10–4 vol. %. Besides the pollution-related aspect, Methane and CO2 are aggressive Greenhouse gas, which, if migrating across the water column into the atmosphere, may affect climate. Evidence for CO2 escape along the fault has not been reported. However, the saturation of the Baltic Sea with CH4 and CO2 is mainly due to the high input of organic substances from rivers (Borges and Abril, 2012), and the amount of gases bound in the water depends on the water temperature (Humborg et al., 2019). It is likely that the amounts of methane produced in Holocene sediments (Spieß, 2012) are significantly larger than the amount that has been released at the location being discussed here. Hence, no impact on the acidification of the Baltic Sea or even on the climate can be inferred from the here discussed fluid escape processes.

6. Conclusions

Shallow gas-escape related features were for the first time identified in the seismic and hydro-acoustic data in Pomeranian Bight, offshore western Poland. Various indicators of gas features including seismic chimneys, bright spots, and acoustic blanking were interpreted on seismic sections with support of seismic attributes. In the area of dominance of near-bottom Quaternary sandy sediments, the gas can leak to the seafloor, forming small (25-35 m diameter) pockmark units. Those shallow gas features are linked with the activity of the Trzebiatów fault zone. We hypothesize that this fault zone is providing potential fluid pathways from Carboniferous or Zechstein formation "kitchen" below to migrate to Upper Triassic sediments or directly to Quaternary shallow sediments, hence explaining the pollution of the Baltic Sea along the Trzebiatów Fault zone by liquid and gaseous hydrocarbon which have been observed during previous studies. Some evidences from the parametric sediment profiler data suggest that after migration, the free gas either accumulates in near seafloor Quaternary sediments or is leaking to the seafloor.

The use of AVO analysis technique in shallow gas investigation is highlighted in this study. AVO attributes analysis proves the presence of remnant free gas in the potential Upper Triassic reservoir (at ~1.15-1.2 s), which supports the hypothesis of gas reservoir existence in the past and the origin of free gas escape to shallow sediments. Our study is probably the first one in which shallow gas can be linked with a potential deeper gas reservoir via AVO analysis.

Our study also proves the potential of hydrocarbon existence in the offshore West Pomerania, which is still considered as poor hydrocarbon exploration area in the Polish territorial waters.

Acknowledgements

This study was funded by the Polish National Science Centre grant no UMO-2017/27/B/ST10/02316. Cruise MSM52 has been funded by German Science Foundation DFG and Federal Ministry of Education

and Research (BMBF). We thank Federal Institute for Geosciences and Natural Resources (BGR) for the license to use seismic data acquired during MSM52 cruise and their support during seismic data acquisition.

We would like to thank IHS Markit Ltd. and GeoSoftware for the donation of academic licenses of Kingdom Suite and Hampson Rusell software packages. Seismic data processing was performed using Globe Claritas package under the academic license from Petrosys Ltd.

We thank the Editor (E. Martorelli), D. Spatola and an anonymous reviewer for helpful comments.

Data availability

Data are available from the authors upon request.

Author contribution statement

Quang Nguyen: Conceptualization, Methodology, Data Curation, Writing – Original Draft preparation, Software, Visualization. **Michal Malinowski**: Supervision, Project administration, Writing – Review & Editing. **Regina Kramarska** and **Dorota Kaulbarsz**: Data Curation, Writing – Original Draft preparation. **Leslaw Mil**: Data Curation. **Christian Hübscher**: Project administration, Funding acquisition, Writing – Review.

Declaration of competing interest

The author declare that they have no known competing financial interests or personal relationships that could have appeared to influence the work reported in this paper.

References

Abegg, F. and Anderson, A.L., 1997. The acoustic turbid layer in muddy sediments of Eckernfoerde Bay, Western Baltic: methane concentration, saturation and bubble characteristics. Marine Geology, 137(1-2), pp.137-147.

Adams, N.J. and Kuhlman, L.G., 1991, November. Shallow gas blowout kill operations. In Middle East Oil Show. OnePetro.

Ahlrichs, N., Hübscher, C., Noack, V., Schnabel, M., Damm, V. and Krawczyk, C.M., 2020. Structural evolution at the northeast North German Basin margin: From initial Triassic salt movement to Late Cretaceous-Cenozoic remobilization. Tectonics, 39(7), p.e2019TC005927.

Ahlrichs, N., Noack, V., Hübscher, C., Seidel, E., Warwel, A. and Kley, J., 2022. Impact of Late Cretaceous inversion and Cenozoic extension on salt structure growth in the Baltic sector of the North German Basin. Basin Research, 34(1), pp.220-250.

Aki, K. and Richards, P.G., 1980. Quantitative seismology, theory and methods, Vol. 1 WH Freeman & Co. New York.

Anderson, A.L. and Bryant, W.R., 1990. Gassy sediment occurrence and properties: Northern Gulf of Mexico. Geo-Marine Letters, 10, pp.209-220.

Bachmann, G.H. and Geluk, M.C., 2010. Chapter 9, Triassic. Petroleum Geological Atlas of the Southern Permian Basin Area. EAGE Publications BV, Houten, 148, p.173.

Brodecka, A., Majewski, P., Bolałek, J. and Klusek, Z., 2013. Geochemical and acoustic evidence for the occurrence of methane in sediments of the Polish sector of the southern Baltic Sea. Oceanologia, 55(4), pp.951-978.

Cartwright, J. and Santamarina, C., 2015. Seismic characteristics of fluid escape pipes in sedimentary basins: implications for pipe genesis. Marine and Petroleum Geology, 65, pp.126-140.

Castagna, J.P. and Swan, H.W., 1997. Principles of AVO crossplotting. The leading edge, 16(4), pp.337-344.

Chopra, S. and Marfurt, K.J., 2007. Seismic attributes for prospect identification and reservoir characterization. Society of Exploration Geophysicists and European Association of Geoscientists and Engineers.

Dadlez, R., 1978. Podpermskie kompleksy skalne w strefie Koszalin–Chojnice. Geological Quarterly, 22(2), pp.269-302.

Dadlez, R., 1980. Tektonika wału pomorskiego. Geological Quarterly, 24(4).

Dadlez, R., Narkiewicz, M., Stephenson, R.A., Visser, M.T.M. and Van Wees, J.D., 1995. Tectonic evolution of the Mid-Polish Trough: modelling implications and significance for central European geology. Tectonophysics, 252(1-4), pp.179-195.

Dadlez, J., 2002. Cyclic sedimentation in the Middle Jurassic of central Poland. Geological Quarterly, 46(3), pp.321-335.

Dadlez, R., 2003. Mesozoic thickness pattern in the Mid-Polish Trough. Geological Quarterly, 47, pp.223-240.

Davy, B., 1992. Seismic reflection profiling on southern lake rotorua-evidence for gas-charged lakefloor sediments. Geothermics, 21(1-2), pp.97-108.

Erlström, M., Thomas, S.A., Deeks, N. and Sivhed, U., 1997. Structure and tectonic evolution of the Tornquist Zone and adjacent sedimentary basins in Scania and the southern Baltic Sea area. Tectonophysics, 271(3-4), pp.191-215.

Fleischer, P., Orsi, T., Richardson, M. and Anderson, A., 2001. Distribution of free gas in marine sediments: a global overview. Geo-Marine Letters, 21(2), pp.103-122.

Floodgate, G.D. and Judd, A.G., 1992. The origins of shallow gas. Continental shelf research, 12(10), pp.1145-1156.

Frahm, L., Hübscher, C., Warwel, A., Preine, J. and Huster, H., 2020. Misinterpretation of velocity pull-ups caused by high-velocity infill of tunnel valleys in the southern Baltic Sea. Near Surface Geophysics, 18(6), pp.643-657.

Frick, M., Kranz, S., Norden, B., Bruhn, D. and Fuchs, S., 2022. Geothermal Resources and ATES Potential of Mesozoic Reservoirs in the North German Basin. Energies, 15(6), p.1980.

Garcia-Gil, S., Vilas, F. and Garcia-Garcia, A., 2002. Shallow gas features in incised-valley fills (Rıa de Vigo, NW Spain): a case study. Continental Shelf Research, 22(16), pp.2303-2315.

Gawenda, P., 2011. Germany–Overview about Renewed Petroleum Activities. AAPG-European Region Newsletter, pp.4-9.

Hilterman, F.J., 2001. Seismic amplitude interpretation. Society of Exploration Geophysicists and European Association of Geoscientists and Engineers.

Hovland, M. and Judd, A.G., 1988. Seabed pockmarks and seepages: impact on geology, biology and the marine environment (Vol. 293). London: Graham & Trotman.

Hovland, M., Judd, A.G. and Burke Jr, R.A., 1993. The global flux of methane from shallow submarine sediments. Chemosphere, 26(1-4), pp.559-578.

Hübscher, C., Ahlrichs, H., Allum, G., Behrens, T., Bülow, J., Krawczyk, C., Damm, V., Demir, Ü., Engels, M., Frahm, L. and Grzyb, G., 2017. BalTec-Cruise No. MSM52–March 1–March 28, 2016–Rostock (Germany)–Kiel (Germany). MARIA S. MERIAN-Berichte, MSM52, 46 pp., DFG-Senatskommission für Ozeanographie.

Hübscher, Christian (2018): Geophysical profiles during Maria S. Merian cruise MSM52. Institut für Geophysik, Universität Hamburg, PANGAEA, https://doi.org/10.1594/PANGAEA.890870

Idczak, J., Brodecka-Goluch, A., Łukawska-Matuszewska, K., Graca, B., Gorska, N., Klusek, Z., Pezacki, P.D. and Bolałek, J., 2020. A geophysical, geochemical and microbiological study of a newly discovered pockmark with active gas seepage and submarine groundwater discharge (MET1-BH, central Gulf of Gdańsk, southern Baltic Sea). Science of The Total Environment, 742, p.140306.

Jakacki, J., Klusek, Z., Têgowski, J. and Warszawy, P., 2002. The non-linear method of gas bubbles detection in the bottom sediments. Revista de Acustica, 33.

Janik, T., Wójcik, D., Ponikowska, M., Mazur, S., Skrzynik, T., Malinowski, M. and Hübscher, C., 2022. Crustal structure across the Teisseyre-Tornquist Zone offshore Poland based on a new refraction/wide-angle reflection profile and potential field modelling. Tectonophysics, 828, p.229271.

Jaśniewicz, D., Klusek, Z., Brodecka-Goluch, A. and Bolałek, J., 2019. Acoustic investigations of shallow gas in the southern Baltic Sea (Polish Exclusive Economic Zone): a review. Geo-Marine Letters, 39(1), pp.1-17.

Jaworowski, K., Wagner, R., Modliski, Z., Pokorski, J., Sokołowski, J. and Sokołowski, A., 2010. Marine ecogeology in semi-closed basin: case study on a threat of geogenic pollution of the southern Baltic Sea (Polish Exclusive Economic Zone). Geological Quarterly, 54(2), pp.267-288.

Jensen, J.B. and Bennike, O., 2009. Geological setting as background for methane distribution in Holocene mud deposits, Århus Bay, Denmark. Continental Shelf Research, 29(5-6), pp.775-784.

Jørgensen, B.B., and Fossing, H., 2012. Methane gas and seismo-acoustic mapping, in: Jørgensen, B.B, Fossing, H., (Eds.), Baltic Gas final scientific report. pp 8-12.

Judd, A.G. and Hovland, M., 1992. The evidence of shallow gas in marine sediments. Continental Shelf Research, 12(10), pp.1081-1095.

Judd, A. and Hovland, M., 2009. Seabed fluid flow: the impact on geology, biology and the marine environment. Cambridge University Press.

Karnkowski, P. H., Pikulski, L. and Wolnowski, T., 2010. Petroleum geology of the Polish part of the Baltic region - an overview. Geological Quarterly, 54 (2), pp.143–158.

Kilhams, B., Kukla, P.A., Mazur, S., McKie, T., Mijnlieff, H.F. and van Ojik, K. eds., 2018, August. Mesozoic resource potential in the Southern Permian Basin. Geological Society of London.

Kim, Y.J., Cheong, S., Chun, J.H., Cukur, D., Kim, S.P., Kim, J.K. and Kim, B.Y., 2020. Identification of shallow gas by seismic data and AVO processing: Example from the southwestern continental shelf of the Ulleung Basin, East Sea, Korea. Marine and Petroleum Geology, 117, p.104346.

Kosakowski, P., Kotarba, M.J., Pokorski, J. and Wróbel, M., 2006, June. Hydrocarbon potential of the Carboniferous strata on the Kołobrzeg and Gryfice blocks (Northwestern Poland). In 68th EAGE Conference and Exhibition incorporating SPE EUROPEC 2006 (pp. cp-2). European Association of Geoscientists & Engineers.

Kotarba, M.J., Kosakowski, P., Więcław, D., Grelowski, C., Kowalski, A., Lech, S. and Merta, H., 2004. Potencjał węglowodorowy karbońskich skał macierzystych w przybałtyckiej części segmentu pomorskiego bruzdy śródpolskiej. Przegląd Geologiczny, 52(12), pp.1156-1165.

Kramarska, R., 1998. Origin and development of the Odra Bank in the light of the geologic structure and radiocarbon dating. Kwartalnik Geologiczny, 42(3), pp.277-288.

Kramarska, R., Krzywiec, P., Dadlez, R., Jegliński, W., Papiernik, B., Przezdziecki, P. and Zientara, P., 1999. Geological map of the Baltic Sea bottom without Quaternary deposits, 1:500 000. Państw. Inst. Geol., Gdańsk-Warszawa.

Kraus, J., Rott, C., and Damte, A., 2018. Tectonic Evolution and Hydrocarbon Exploration of a Multiple Overprinted Caledonian Continental Collision Zone in the German Baltic Sea. Search and Discovery Article #11064 (2018).

Krzywiec, P., 2002. The Oświno structure (NW Mid-Polish Trough)-salt diapir or inversion-related compressional structure?. Geological Quarterly, 46, pp.337-346.

Krzywiec, P., Kramarska, R. and Zientara, P., 2003. Strike-slip tectonics within the SW Baltic Sea and its relationship to the inversion of the Mid-Polish Trough—evidence from high-resolution seismic data. Tectonophysics, 373(1-4), pp.93-105.

Krzywiec, P., 2006. Structural inversion of the Pomeranian and Kuiavian segments of the Mid-Polish Trough--lateral variations in timing and structural style. Geological Quarterly, 50(1), pp.151-168.

Krzywiec, P., Stachowska, A., Grzybowski, L., Nguyen, Q., Słonka, L., Malinowski, M., Kramarska, R., Ahlrichs, N., Hübscher, C., 2022. The Late Cretaceous inversion of the Polish Basin and surrounding area – a current perspective based on seismic data, In book: Cretaceous of Poland and of adjacent areas. Field trip guides. 11th International Cretaceous Symposium, Warsaw, Poland. Publisher: Faculty of Geology, University of Warsaw.

Laier, T. and Jensen, J.B., 2007. Shallow gas depth-contour map of the Skagerrak-western Baltic Sea region. Geo-Marine Letters, 27(2), pp.127-141.

Majewski, P. and Klusek, Z., 2011. Expressions of shallow gas in the Gdansk Basin. Zeszyty naukowe Akademii Marynarki Wojennej, 52, pp.61-71.

Majewski, P. and Klusek, Z., 2014. Parameters of echo signals originated from a gas seepage site in the southern Baltic Sea. Hydroacoustics, 17, pp.143–150.

Marfurt, K.J., Kirlin, R.L., Farmer, S.L. and Bahorich, M.S., 1998. 3-D seismic attributes using a semblance-based coherency algorithm. Geophysics, 63(4), pp.1150-1165.

Marfurt, K.J., 2018. Seismic attributes as the framework for data integration throughout the oilfield life cycle. Society of Exploration Geophysicists.

Mathys, M., Thiessen, O., Theilen, F., Schmidt, M., 2005. Seismic characterization of gas-rich near surface sediments in the Arkona Basin, Baltic Sea. Marine Geophysical Researches, 26, pp.207–224.

Meldahl, P., Heggland, R., Bril, B. and de Groot, P., 1999. The chimney cube, an example of semi-automated detection of seismic objects by directive attributes and neural networks: Part I; methodology. In SEG Technical Program Expanded Abstracts 1999 (pp. 931-934). Society of Exploration Geophysicists.

Naudts, L., De Batist, M., Greinert, J. and Artemov, Y., 2009. Geo-and hydro-acoustic manifestations of shallow gas and gas seeps in the Dnepr paleodelta, northwestern Black Sea. The Leading Edge, 28(9), pp.1030-1040.

Nguyen Q, 2020, Seismic Data Processing Report (BALTEC / MSM52). Institute of Geophysics PAS. https://dspace.igf.edu.pl/xmlui/handle/123456789/112.

668 Pan, Y., Seidel, E., Juhlin, C., Hübscher, C. and Sopher, D., 2022. Inversion tectonics in the Sorgenfrei–
669 Tornquist Zone: insight from new marine seismic data at the Bornholm Gat, SW Baltic Sea. GFF, 144(2),
670 pp.71-88.

671 Parkes, R.J., Cragg, B.A., Fry, J.C., Herbert, R.A. and Wimpenny, J.W.T., 1990. Bacterial biomass and activity
672 in deep sediment layers from the Peru margin. Philosophical Transactions of the Royal Society of London. Series
673 A, Mathematical and Physical Sciences, 331(1616), pp.139-153.

674 Pernille-1 unpublished well report, 1989.

675 Pokorski, J., 2010. Geological section through the lower Paleozoic strata of the Polish part of the Baltic
676 region. Geological Quarterly, 54(2), pp.123-130.

677 Ren, S., Liu, Y., Huang, F. and Zhang, P., 2019. Quantitative Classification of Shallow Gas Blowout during
678 Offshore Drilling Process. Journal of Petroleum & Environmental Biotechnology, 10(393), pp.1-6.

679 Russell, B.H., Lines, L.R. and Ross, C.P., 2002. AVO classification using neural networks: A comparison
680 of two methods. CREWES Res. Rep., 14, pp.1-18.

681 Schäfer, W., Hübscher, C., Sopher, D., 2021. Seismic stratigraphy of the Klints Bank east of Gotland (Baltic
682 Sea): A giant drumlin sealing thermogenic hydrocarbons. Geo-Marine Letters 41:9,
683 doi.org/10.1007/s00367-020-00683-3.

684 Scheck-Wenderoth, M. and Lamarche, J., 2005. Crustal memory and basin evolution in the Central
685 European Basin System—new insights from a 3D structural model. Tectonophysics, 397(1-2), pp.143-165.

686 Schlüter, H.U., Best, G., Jürgens, U. and Binot, F., 1997. Interpretation reflexionsseismischer Profile
687 zwischen baltischer Kontinentalplatte und kaledonischem Becken in der südlichen Ostsee-erste Ergebnisse.
688 Zeitschrift der deutschen geologischen Gesellschaft, pp.1-32.

689 Schroot, B.M. and Schüttenhelm, R.T., 2003. Shallow gas and gas seepage: expressions on seismic and
690 otheracoustic data from the Netherlands North Sea. Journal of Geochemical Exploration, 78, pp.305-309.

691 Schroot, B.M. and Schüttenhelm, R.T.E., 2003. Expressions of shallow gas in the Netherlands North Sea.
692 Netherlands Journal of Geosciences, 82(1), pp.91-105.

693 Schroot, B.M., Klaver, G.T. and Schüttenhelm, R.T., 2005. Surface and subsurface expressions of gas
694 seepage to the seabed—examples from the Southern North Sea. Marine and Petroleum Geology, 22(4),
695 pp.499-515.

696 Simm, R., Bacon, M. and Bacon, M., 2014. Seismic amplitude: An interpreter's handbook. Cambridge
697 University Press.

698 Singh, D., Kumar, P.C. and Sain, K., 2016. Interpretation of gas chimney from seismic data using artificial
699 neural network: A study from Maari 3D prospect in the Taranaki basin, New Zealand. Journal of Natural
700 Gas Science and Engineering, 36, pp.339-357.

701 Stina-1 unpublished well report, 1989.

Sullivan, E.C., Marfurt, K.J., Lacazette, A. and Ammerman, M., 2006. Application of new seismic attributes to collapse chimneys in the Fort Worth Basin. Geophysics, 71(4), pp.B111-B119.

Tęgowski, J., Jakacki, J., Klusek, Z., Rudowski, S., 2003. Nonlinear acoustical methods in the detection of gassy sediments in the Gulf of Gdańsk. Hydroacoustics, 6, pp.151–158.

Thießen, O., Schmidt, M., Theilen, F., Schmitt, M. and Klein, G., 2006. Methane formation and distribution of acoustic turbidity in organic-rich surface sediments in the Arkona Basin, Baltic Sea. Continental Shelf Research, 26(19), pp.2469-2483.

Tóth, Z., Spieß, V. and Jensen, J., 2014. Seismo-acoustic signatures of shallow free gas in the Bornholm Basin, Baltic Sea. Continental Shelf Research, 88, pp.228-239.

Tóth, Z., Spiess, V. and Keil, H., 2015. Frequency dependence in seismoacoustic imaging of shallow free gas due to gas bubble resonance. Journal of geophysical research: solid earth, 120(12), pp.8056-8072.

Vejbaek, O.V., Stouge, S. and Damtoft Poulsen, K., 1994. Palaeozoic tectonic and sedimentary evolution and hydrocarbon prospectivity in the Bornholm area.

Wagner, R., 2011. Natural migration of liquid and gaseous subsurface hydrocarbons into bottom sediments and waters. In: Uścinowicz, S. (Ed.), Geochemistry of Baltic Sea surface sediments. Polish Geological Institute - National Research Institute, Warsaw, pp. 125–145.

Zimmermann, J., Franz, M., Heunisch, C., Luppold, F.W., Mönnig, E. and Wolfgramm, M., 2015. Sequence stratigraphic framework of the Lower and Middle Jurassic in the North German Basin: Epicontinental sequences controlled by Boreal cycles. Palaeogeography, Palaeoclimatology, Palaeoecology, 440, pp.395-416.